tional Committee for Physical Sciences of the Italian National Research Council (CNR).

Joseph Quartieri was born in Gioiosa Ionica (Reggio Calabria), Italy, in 1950. He received the Dr. Degree (summa cum laude) in physics from the University of Naples, Naples, Italy, in 1975 and then remained a few years to do research in the area of laser modeling and applications. In 1977 and 1978 he was awarded two fellowships from the Fiat Research Center, (ATA), Orbassano, Italy.

For the past five years he has been teaching Physics and Mathematics at the Engineering Faculty of the University of Naples. At the same time he has been working as a researcher for the CNR on the Italian High Power Laser Finalized Project. At present he is working both at the University of Naples and at the CNR Cybernetics Institute, Arco Felice, Naples, Italy. His scientific interests range from biological and medical applications of lasers to some new fields of applied mathematics involving computational techniques.

High Intensity Effects in Biological and Medical Samples*

AARON J. DAGEN, ROBERT R. ALFANO, AND CHARLES E. SWENBERG, MEMBER, IEEE

Abstract—Intense excitation sources are known to cause nonlinear optical effects in biological samples. Similarly, high power lasers, used as medical and surgical tools, can induce nonlinear processes in tissues. In this paper we describe and research the theory of one such high intensity effect: bimolecular singlet–singlet exciton annihilation.

I. INTRODUCTION

THE interaction of high intensity optical laser radiation with biological samples is of interest to both the medical and biological communities. Lasers have been extensively used for surgical and medical treatments of pathological tissues in humans and for analysis of chemical and physical changes in biological samples. On a molecular scale, high intensity photon beams delivered on a short time scale result in additional mechanisms that do not occur under low intensity excitation. These processes include multiple photon absorption, ground state depletion, upper excited state absorption, and bimolecular fusion of excited electronic states. In order to evaluate the efficacy of any technique using high intensity pulses it is necessary to understand and quantitate the nonlinear processes occurring.

For photosynthetic samples it is well known that singlet–singlet exciton annihilation reactions occur at high intensities. Typically, the onset of nonlinear alterations in measurable observables such as the fluorescence yield occur at a photon excitation fluence of 1×10^{14} photons cm^{-2} [1]-[9]. The importance of this particular bimolecular interaction in probing photosynthetic membranes has resulted in the development of a general theory of exciton fusion in small domains. Both the fluorescence kinetic profiles and the relative fluorescence yields as a function of laser excitation intensity provide a direct measure of the bimolecular rate constant. It is not unreasonable to expect that the exciton fusion process should occur in other biological samples upon excitation by high intensity laser pulses. This paper describes, in detail, the Paillotin-Swenberg exciton annihilation theory and presents computer generated curves of fluorescence kinetics and quantum yield for a variety of energy migration domains and source intensities. These curves should be valuable to those attempting to ascertain if bimolecular processes are occurring in their biological and medical samples under photoexcitation.

II. THEORY

The Paillotin-Swenberg annihilation theory is the most comprehensive description of the fluorescence temporal decay curves $F(t)$ and fluorescence quantum yield ϕ obtained from systems in which bimolecular, as well as monomolecular decay processes occur [4], [10]. No assumptions are made concerning the actual dimensions of the domain size where the excitons are mobile. The theory does not include the effects of ground state depletion and upper excited state absorption.

Thus, the predictions of the theory are highly inaccurate in cases where the number of molecules excited are a significant fraction of the total number of molecules in the domain. If exciton fusion is the dominant nonlinear process then the theory does allow one to estimate domain size from a comparison of theoretically calculated and experimentally obtained quantum fluorescent yield and fluorescence kinetic curves. In addition to reducing to Swenberg theory [4] for very large domains, and the Mauzerall theory [1], [5] for very small domains, the theory in appropriate limits predicts decay curves which can be fitted to time dependent decays of the form $\exp(-bt^{1/2} - kt)$. During the course of our research, we found intensity ranges and domain sizes which give decays which can be fitted to the function $\exp(-bt^{1/3} - kt)$. Decays of this function form are expected from aggregated molecules, with fluorescence lifetimes $\tau = 1/k$, which transfer energy to each other and are randomly located in an infinite lattice. The $t^{1/2}$ decay law is appropriate for a three-dimensional lattice and a $t^{1/3}$ decay law holds when migration is restricted to a two-dimensional lattice.

The Paillotin et al. [10] theory considers an aggregated collection of molecules called a domain within which energy migration and annihilation can occur. Let i denote the number of excitons in any given domain at time t. These excitations decay in time by monomolecular, as well as bimolecular processes. The theory examines the probability $p_i(n,t)$ of there being i excitons in the domain at time t, given that there were n excitons created at time $t = 0$. In the special case where the domain size can exist without physical constraints, i.e., where physical size is limited only by the nearest neighbor transfer rate and the excited state lifetime, the family of coupled differential equations for $p_i(n,t)$ can be solved in closed form. If $\langle i(t)\rangle_n$ denotes the average number of excitons at time t, given that n excitons were created at time $t = 0$, then the fluorescence $F_n(t)$ from this domain is proportional to $\langle i(t)\rangle_n$ and the fluorescence quantum yield is proportional to the integral of $F_n(t)$.

In an actual experiment, one can only determine the average number of excitons y created at time $t = 0$. The average number of excitons created is related to the pulse intensity I by

$$y = \sigma I \tag{1}$$

where σ is the absorption cross section. Equation (1) defines the absorption cross section and reflects the fact that a laser pulse of intensity I incident on many similar domains actually creates a different number of excitons in each domain. When the domain size is not limited by physical boundaries the number of excitons within a given domain at time $t = 0$ is governed by Poisson statistics [11], [12]. Thus the probability of having n excitons within a domain is

$$P(n/y) = y^n e^{-y}/n! \tag{2}$$

if y is the average number of excitons created at time $t = 0$. When the number of molecules M forming a domain is small, then a binominal distribution is more appropriate. If P_0 denotes the probability that a molecule is in an excited state, then the probability that a domain contains k excitons at time $t = 0$ is

$$B_M(k,P_0) = \frac{M!}{(M-k)!\,k!}\, P_0^k (1-P_0)^{M-k} \tag{3}$$

where $y = MP_0$.

For photosynthetic membranes the experimental situation meets the criteria appropriate for Poisson statistics [10]. The expressions for $F_n(t)$ and ϕ_n are therefore weighted by that distribution in order to obtain the observed fluorescence decay $F(t)$ and quantum yield ϕ, i.e.,

$$F(t) = y^{-1} \sum_{n=0}^{\infty} P(n/y)\, nF_n(t) \tag{4a}$$

$$\phi = y^{-1} \sum_{n=0}^{\infty} P(n/y)\, n\phi_n. \tag{4b}$$

Equations (4a) and (4b) describe the actual experimental condition: a certain probability exists that there will be n excitons created at time $t = 0$ given that y is the average number of excitons created. This probability is multiplied by the fluorescence and quantum yields, $F_n(t)$ and ϕ_n, that result in the particular situation where n excitons are created at $t = 0$. Each product is in turn multiplied by the number of excitons n to create the weighted average of ϕ_n and $F_n(t)$ that are experimentally observed. When the constraints of the domain are fixed by a finite number of molecules M, (4a) and (4b) are replaced by

$$F(t) = \sum_{n=1}^{M} \frac{(M-1)!}{(n-1)!\,(M-n)!}\, P_0^{n-1}(1-P_0)^{M-n}\, F_n(t) \tag{5a}$$

where

$$F_n(t) = n^{-1} \sum_{k=1}^{n} k p_k(n,t) \tag{5b}$$

and ϕ is proportional to the integral of $F(t)$.

In developing the differential equation from which expressions for the physical observables are obtained, often called the master equation because deriving the correct results is dependent on and hence subservient to writing the correct equation, the theory makes the following assumptions.
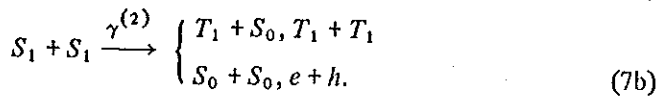
1) The exciton distribution randomization time is very short and is smaller than the characteristic exciton annihilation time.

2) The depletion of ground state molecules is negligible.

3) The exciton coherence time is extremely short so that memory effects can be neglected.

4) There are no chemical reactions. For photosynthesis this corresponds to assuming all reaction centers are closed.

5) Upper excited state absorption and multiple photon absorption are neglected.

The state of a particular domain is defined by the number (i) of excitons it contains at a particular time (t). These (i) excitons decay in time by both radiative and nonradiative processes. The monomolecular processes are characterized by the

rate constant K where

$$K = k_f + k_{is} + k_D. \tag{6}$$

k_f is the radiative decay constant, k_{is} is the intersystem cross-over rate constant, and k_D is a nonradiative term describing the decay from the first excited singlet S_1 to the ground state S_0. In addition to monomolecular processes, the excitons decay through bimolecular processes. In a domain in which several excitons migrate, the most significant bimolecular deactivation process is singlet–singlet exciton annihilation. Annihilation is the interaction of two molecules, both initially in the first excited state, which results in either one or both molecules decaying to a lower triplet or ground state or in the production of ion pairs (e, h). These processes can be characterized by two rate constants $\gamma^{(1)}$ and $\gamma^{(2)}$ where

$$S_1 + S_1 \xrightarrow{\gamma^{(1)}} S_1 + S_0 \tag{7a}$$

$$S_1 + S_1 \xrightarrow{\gamma^{(2)}} \begin{cases} T_1 + S_0, T_1 + T_1 \\ S_0 + S_0, e + h. \end{cases} \tag{7b}$$

T_1 denotes the lowest triplet state, and e and h represent the lowest anion and cation states of the molecule. The last process in (7b) occurs only if the internal ionization threshold is lower than twice the lowest excited singlet state energy. For biological systems this route of decay can be quite significant since following ionization molecular bond breakage is a likely pathway.

When the number of pairwise interactions that (i) excitons can have is taken into account, the decay of an (i) state to an $(i - \alpha)$ state for $\alpha = 1, 2$ is described by

$$T^\alpha(i \to i - \alpha) = i(i - 1) \gamma^{(\alpha)}/2. \tag{8}$$

The monomolecular decay rate for a state of i excitons is given simply by

$$T^m(i \to 1) = Ki \tag{9}$$

where K is described in (6). It describes the probability of i exciton states decaying to $i - 1$ exciton states due to monomolecular processes.

For a delta function excitation pulse at time $t = 0$, the differential equation for $p_i(n, t)$ is

$$\frac{dP_i(n, k)}{dt} = k(i + 1) p_{i+1}(n, t) - Kip_i(n, t)$$
$$+ \left\{ \gamma^{(1)} \frac{i(i + 1)}{2} p_{i+1}(n, t_1) \right.$$
$$+ \gamma^{(2)} \frac{(i + 1)(i + 2)}{2} p_{i+2}(n, t) \right\}$$
$$- \left\{ \gamma^{(1)} \frac{i(i - 1)}{2} + \gamma^{(2)} \frac{i(i - 1)}{2} \right\} p_i(n, t). \tag{10}$$

The first two terms describe the monomolecular decay. The third and fourth terms describe the source and decay channels resulting from biomolecular processes in which either one or both excitons are deactivated; $(i + 1)$ and $(i + 2)$ states feed the (i) states, while the (i) states decay to $(i - 1)$ and $(i - 2)$ states. The average number of excitons at time t for a state

having n excitons initially is defined as

$$\langle i(t) \rangle_n = \sum_{i=1}^{n} i \, p_i(n, t). \tag{11}$$

With this definition Paillotin et al. [10] have shown that the continuum limit solution (7) is recovered from (10) in the limit of large domains. Thus

$$\frac{d \langle i \rangle_n}{dt} = -K \langle i \rangle_n - (\gamma^{(2)} + \gamma^{(1)})/2 \langle i(i - 1) \rangle_n \tag{12a}$$

$$\approx -K \langle i \rangle_n - (\gamma^{(2)} + \gamma^{(1)})/2 \langle i \rangle_n^2 \tag{12b}$$

in the limit, where the exciton density can be treated as a continuous variable, $\langle i(i - 1) \rangle_n \approx \langle i \rangle_n^2$. This case is identical to the Swenberg continuum model [2], [4], [13].

For unrestricted domain sizes $(M \to \infty)$ analytical expressions for $F(t)$ and ϕ, the microscopic observables are readily obtained from the generating function solutions of (10). Paillotin and co-workers [10] have shown that

$$F(t) = \sum_{p=0}^{\infty} A_P(-1)^p \exp \{-(p + 1)(p + r) \tau\} \tag{13}$$

where

$$\tau = (\gamma^{(1)} + \gamma^{(2)})t/2,$$

$$A_P = \sum_{k=P}^{\infty} \frac{(-1)^k \, k! Z^k (r + 1 + 2p)}{p! \, (k - p)! \, (r + p + 1) \cdots (r + p + k + 1)} \tag{14}$$

and

$$\phi/\phi_0 = r \sum_{k=0}^{\infty} (-1)^k Z^k / r(r + 1) \cdots (r + k)(k + 1) \tag{15}$$

where ϕ_0 is the fluorescence quantum yield at low laser excitation intensities. The parameters used in (14) and (15) are defined as

$$\gamma = \gamma^{(1)} + \gamma^{(2)}, r = 2K/\gamma, \xi = \gamma^{(2)}/\gamma, Z = y(1 + \xi), y = \sigma I \tag{16}$$

where γ is the total bimolecular rate due to one or both excitons decaying to lower energy levels and r is the ratio of twice the monomolecular decay rate to the total bimolecular decay constant, and is thus related to domain size. For unrestricted large domains, the Swenberg limit, $\gamma \ll 2K$, holds because the volume over which excitons migrate dominates the monomolecular decay processes. As a result, $r \to \infty$ corresponds to the large domain, continuum limit. In a small domain, where the confinement crowds the excitons and thereby increases the chances of annihilation, the bimolecular processes dominate; $2K \ll \gamma$. This limit, described by $r \to 0$, is similar to the conditions assumed by Mauzerall [1], [5]. y is the average number of hits per domain, or the average number of excitons created at $t = 0$. Z is therefore proportional, within a factor of 2, to the number of hits per domain.

It is comforting to note that the unrestricted domain expressions for $F(t)$ and ϕ/ϕ_0 reduce to the relationships ex-
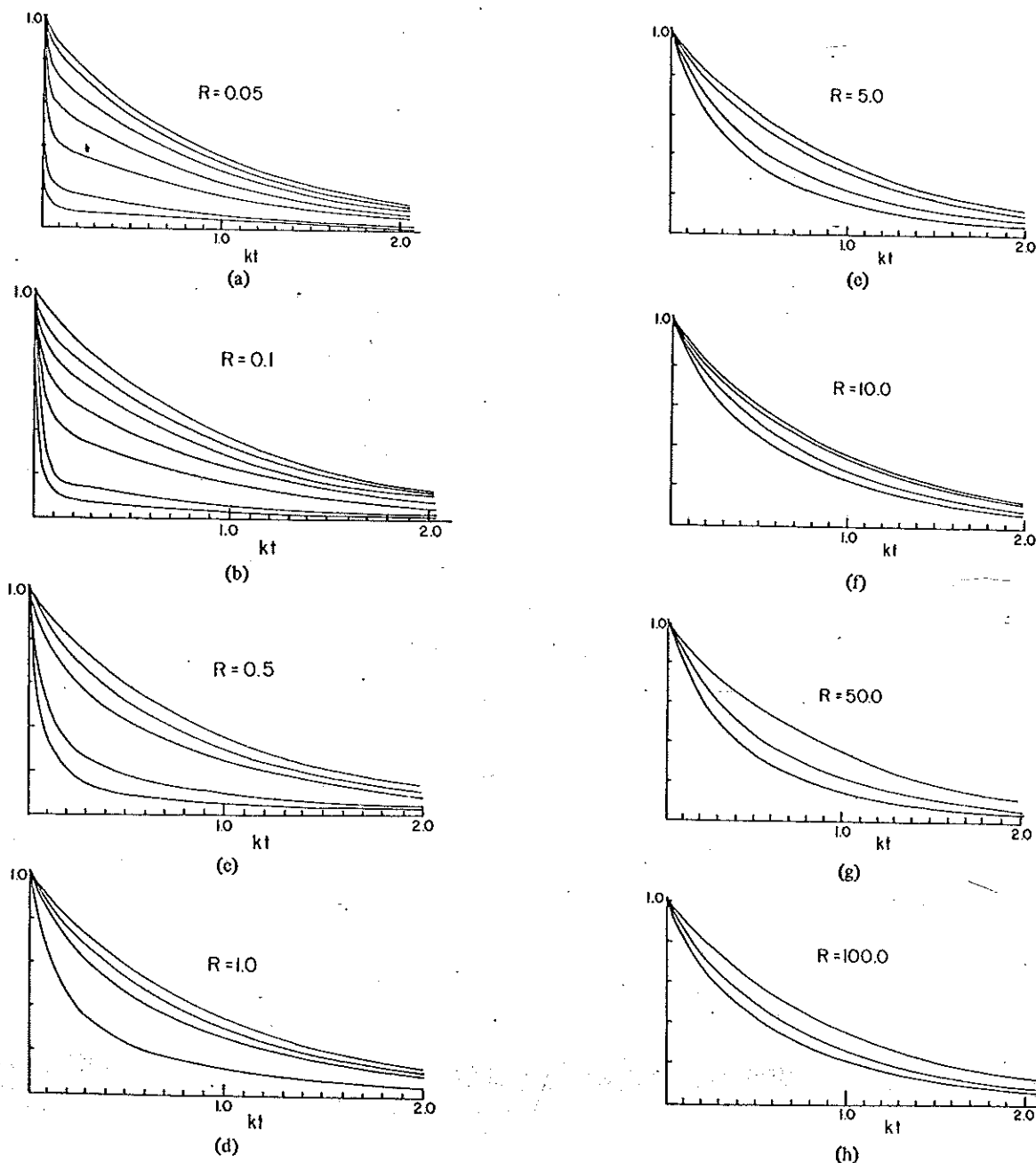
Fig. 1. Fluorescence curves for representative values of R and Z versus Kt in annihilation theory. In descending order (a) $r = 0.05$, $Z = 0.1$, 0.2, 0.5, 1.0, 2.0, 5.0, 10.0; (b) $r = 0.1$, $Z = 0.005$, 0.2, 0.5, 1.0, 2.0, 5.0, 10.0; (c) $r = 0.5$, $Z = 0.05$, 0.5, 1.0, 5.0, 10.0; (d) $r = 1.0$, $Z = 0.05$, 0.5, 1.0, 5.0; (e) $r = 5.0$, $Z = 0.05$, 1.0, 5.0, 10.0; (f) $r = 10.0$, $Z = 0.05$, 1.0, 5.0, 10.0; (g) $r = 50.0$, $Z = 5.0$, 50,0, 100.0; (h) $r = 100.0$, $Z = 5.0$, 50.0, 100.0.

pected in the appropriate limits.

$$F(t) = \{e^{Kt}(1 + Z/r) - Z/r\}^{-1}, \quad \phi/\phi_0 = \frac{r}{Z} \ln \{1 + Z/r\} \quad (17)$$

for $r \to \infty$ limit, and

$$F(t) = (1 - e^{-Z}) e^{-Kt}/Z, \quad \phi/\phi_0 = (1 - e^{-Z})/Z \quad (18)$$

in the small domain, $r \to 0$ limit. The bimolecular rate constant $\bar{\gamma}$ that usually appears in second order kinetic analysis is related to that given in (16) by the appropriate volume of the domain, i.e., $\bar{\gamma} = V\gamma$.

III. ANALYSIS

Equations (14) and (15) were used to generate the theoretical curves for $F(t)$ and ϕ/ϕ_0. The terms in the expression for the coefficients A_p can easily be shown to be monotonically decreasing. By truncating each sum when the last term is less than 10^{-17}, we obtain accuracies much better than the two digit accuracy we report. In most cases, a 15 term exponential is more than enough to accurately generate the curve. Similarly, the values of ϕ/ϕ_0 as a function of Z were obtained by truncating the sum after the last term was less than 10^{-17}.

The curves for representative values of r and Z are shown in Figs. 1 and 2. Table I lists the coefficients A_p used in the
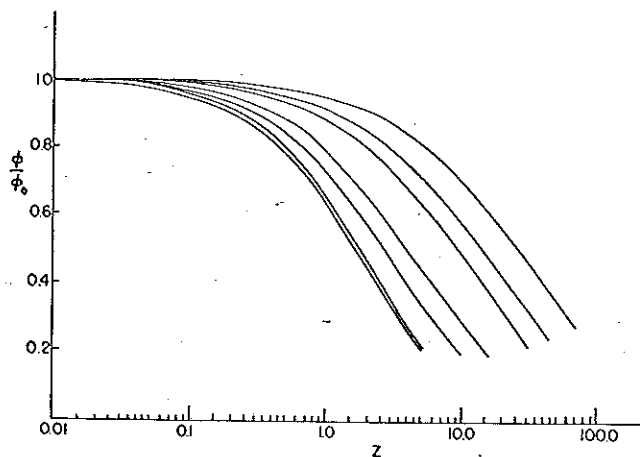
Fig. 2. Quantum yield ϕ/ϕ_0 versus number of hits Z. Curves for smaller values of r break sooner. The curves shown are for $r = 0.05, 0.1, 0.5, 1.0, 3.0, 5.0, 10.0$.

TABLE 1
MAGNITUDE OF COEFFICIENTS A_p IN EXPRESSION FOR $F(t)$ LISTED VERSUS R AND Z

R	Z	A_0	A_1	A_2	A_3	A_4	A_5	A_6
.05	.001	.9995	.0005					
.05	.100	.953	.046	.00077				
.05	.500	.792	.192	.015				
.05	1.00	.639	.305	.050	.005			
.05	5.00	.206	.365	.259	.118	.039	.011	.002
.05	10.00	.104	.242	.259	.194	.113	.054	.022
.100	.005	.9976	.0023					
.100	.100	.954	.045					
.100	.500	.796	.180	.065				
.100	1.0	.646	.2996	.049	.005			
.100	5.0	.213	.364	.256	.116	.039	.010	.02
.100	10.0	.109	.243	.258	.192	.112	.054	.02
.500	.05	.980	.02					
.500	.50	.823	.161	.013	—			
.500	1.00	.693	.262	.041	.004			
.500	5.00	.265	.357	.233	.101	.033	.008	
.500	10.00	.142	.254	.250	.179	.101	.047	.01
1.0	.05	.984	.016					
1.0	.50	.852	.137	.010				
1.0	1.00	.736	.228	.033	.003			
1.0	5.00	.321	.349	.208	.086	.027	.007	.001
1.0	10.00	.180	.264	.240	.163	.087	.041	.011
5.0	.05	.993	.007					
5.0	.50	.933	.064	.003				
5.0	1.0	.873	.115	.011	.001			
5.0	5.0	.569	.282	.107	.032	.008	.002	
5.0	10.0	.390	.289	.174	.087	.038	.014	
10.0	.05	.996	.004					
10.0	.50	.960	.039	.013				
10.0	1.00	.923	.073	.005				
10.0	5.0	.701	.223	.059	.014	.003		
10.0	10.0	.536	.273	.121	.047	.016	.005	.001
50.0	0.05	.999	.001					
50.0	1.0	.981	.019					
50.0	5.0	.912	.081	.007	.001			
50.0	10.0	.838	.137	.021	.003			
50.0	50.0	.507	.256	.126	.060	.028	.013	
50.0	100.0	.339	.231	.155	.102	.065	.042	.026
100.0	1.0	.9995	.0004					
100.0	5.0	.953	.045	.062				
100.0	10.0	.911	.082	.007				
100.0	50.0	.670	.222	.073	.023			
100.0	100.0	.504	.253	.126	.061	.029	.014	

temporal fluorescence profiles for representative values of r and Z. For each value of r corresponding to a particular domain size, the fluorescence is best described by a single exponential for small values of Z; the exact value of Z for a single exponential fit depends on r. As Z increases, for each value of r, the decay becomes more nonexponential, as expected. Examination of the theoretical curves shows the decay curves, for each value of r, are noticeably sensitive to changes in Z. Quantum yield curves have basically the same shape for $r > 5$, but the shapes of the quantum yield curves are quite sensitive to changes in r for $r < 1$. It has been shown that for $r = 2$-5, fluorescence kinetics curves correspond to the $e^{-a\sqrt{t}}$ decay law. The fluorescence curves for $r = 0.05$-0.5 can be fit to curves of the form $e^{-at^{1/3} - kt}$. These relationships are displayed in Fig. 3(a) and (b). When the number of molecules in the domain is small and finite the fluorescence decay and quantum yield must be computed using (5a) and (5b). The relation quantum yield versus average number of hits y for domains with $M = 4$ and 100 is shown in Fig. 4. Obviously, for $y \geq M$, $\phi(y)$ is meaningless. It should also be apparent that for y near M, other nonlinear processes (ones not included in the formalism developed here) are dominant. The calculation reported in Fig. 4 illustrates that ϕ versus y, at least for $\gamma^{(2)} = 0$ and $r = 1.0$, is quite insensitive to M. The calculated fluorescence decays $F(t)$ show no discernible differences for those values of M.

The $t^{1/2}$ and $t^{1/3}$ decay laws can also be explained, respectively, by a three- or two-dimensional infinite lattice containing randomly located fluorescing molecules. To ascertain that annihilation processes are occurring, and that the Paillotin-Swenberg theory is appropriate as opposed to a different model yielding similar results, quantum yield measurements must be taken in addition to obtaining the temporal decay profiles as a function of intensity. We have used a photomultiplier integrator system to obtain quantum yield measurements. The accuracy and simplicity of the system, which gives one the ability to take many shots in each intensity range, results in extremely small error bars in the measurements. Such accurate results can then be fit to the theory to find the appropriate value of r for the system, and the value of Z corresponding to a given value of I. As explained previously, Z is proportional to I, and while experimental results are plotted against I, the theoretical curves are plotted against Z. After fitting the curves, the decay kinetics can be fit at different intensities. These curves can be measured with either a streak camera, photon-counting phase delay technique, or a photomultiplier-oscilloscope arrangement depending on whether the temporal resolution required is 2 ps, 200 ps, or 1 ns, respectively [14], [15]. It is necessary that experiments
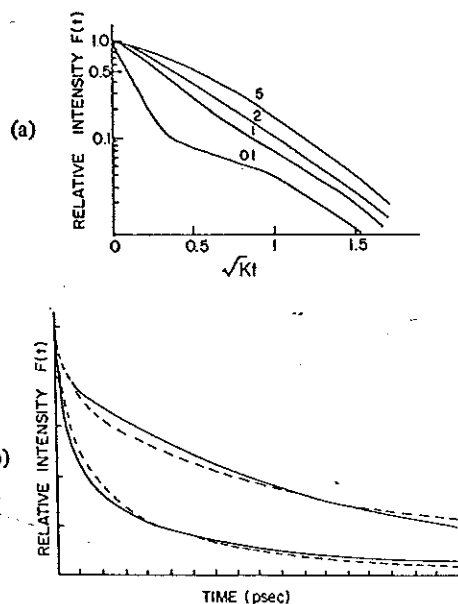
≈. 3. (a) Plot of log $F(t)$ versus $\sqrt{kt}$ for $Z = 10$ and representative r values showing resemblance of $r = 2\text{-}5$ curves to $\sqrt{t}$ decay law. (b) Plot of annihilation theory curves (solid lines) and $F(t) = \exp(-at^{1/3} - kt)$ curves (dashed curves) versus time in picoseconds. Upper curve: Solid: $r = 0.05$, $Z = 0.5$, $k = 7.5 \times 10^8$ s^{-1}; dashed: $a = 0.63 \times 10^3$ $s^{-1/3}$, $k = 3.75 \times 10^8$ s^{-1}. Laser curve: Solid, $r = 0.5$, $z = 5.0$, $k = 1 \times 10^9$ s^{-1}; dashed: $a = 1.43 \times 10^3$ $s^{-1/3}$, $k = 1.0 \times 10^9$ s^{-1}.
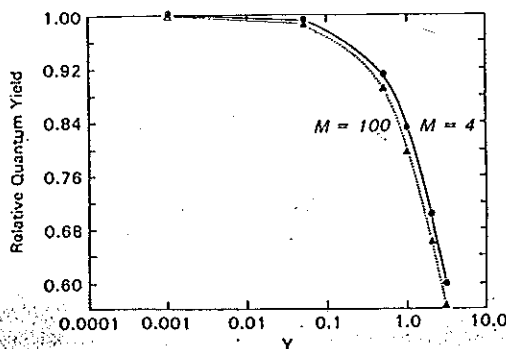

Fig. 4. The relative fluorescence quantum yield versus the average number of hits Y for $M = 4$ and 100; calculated using (5a) and (5b) for $r = 1.0$ and $\gamma^{(2)} = 0$.

also measure transmission data versus intensity. This ensures that a drop in quantum yield is due to annihilation processes and not bleaching.

IV. CONCLUSION

Lasers have become a popular tool in the medical profession, while at the same time they have been shown to cause nonlinear processes not ordinarily found in nature. The importance of ti ;c   ..   .cit   . . . . in the development of a general theory describing it, and experimental techniques for determining its existence. A general theory of fluorescence decay and fluorescence quantum yield which includes ground state depletion and upper excited state absorption in addition to exciton fusion is still lacking.

REFERENCES

[1] D. Mauzerall, "Multiple excitations in photosynthetic systems," *Biophys. J.*, vol. 16, pp. 87–93, 1976.
[2] A. J. Campillo, S. L. Shapiro, V. H. Kollman, K. R. Winn, and R. C. Hyer, "Picosecond exciton annihilation in photosynthetic systems," *Biophys. J.*, vol. 16, pp. 93–96, 1977.
[3] A. J. Campillo, V. H. Kollman, and S. L. Shapiro, "Intensity dependence of the fluorescence lifetime of *in vivo* chlorophyll excited by a picosecond light pulse," *Science*, vol. 193, p. 227, 1976.
[4] C. E. Swenberg, N. E. Geacintov, and M. Pope, "Bimolecular quenching of excitons and fluorescence in the photosynthetic unit," *Biophys. J.*, vol. 16, p. 1447, 1976.
[5] D. Mauzerall, "Fluorescence and multiple excitation in photosynthetic systems," *J. Phys. Chem.*, vol. 80, pp. 2306–2310, 1976.
[6] G. Porter, C. J. Tredwell, G. F. W. Searle, and J. Barber, "Picosecond time-resolved energy transfer in phorphyridium cruentum," *Biochim. Biophys. Acta*, vol. 501, pp. 232–253, 1978.
[7] G. F. W. Searle, J. Barber, L. Harris, G. Porter, and C. J. Tredwell, "Picosecond laser study of fluorescence lifetimes in spinach chloroplast photosystem I and photosystem II preparations," *Biochim. Biphys. Acta*, vol. 459, pp. 390–401, 1977.
[8] D. F. Wong, F. Pellegrino, R. R. Alfano, and B. A. Zilinskas, "Fluorescence relaxation kinetics and quantum yield from the isolated phycobiliproteins of the blue-green *Alga nostoc sp.* measured as a function of single picosecond pulse intensity," *Photochem. Photobiol.*, vol. 33, pp. 651–662, 1981.
[9] A. G. Doukas, V. Stefancic, J. Buchert, R. R. Alfano, and B. A. Zilinskas, "Exciton annihilation in the isolated phycobiliproteins from the blue-green *Alga nostroc sp.* using picosecond absorption spectroscopy," *Photochem, Photobiol.*, vol. 34, pp. 505–510, 1981.
[10] G. Paillotin, C. E. Swenberg, J. Breton, and N. E. Geacintov, "Analysis of picosecond laser-induced fluorescence phenomena in photosynthetic membranes utilizing a master equation approach," *Biophys. J.*, vol. 25, pp. 513–523, 1979.
[11] R. V. Hogg and A. T. Craig, *Introduction to Mathematical Statistics*, 4th ed. New York: Macmillan, 1978.
[12] A. C. Melissinos, *Experiments in Modern Physics*. New York: Academic, 1966.
[13] C. E. Swenberg and N. E. Geacintov, in *Organic Molecular Photophysics*, J. B. Birks, Ed. Sussex, England: Wiley, 1973.
[14] N. H. Schiller, A. J. Dagen, and R. R. Alfano, "A method to calibrate streak cameras," *Photonics Spectra*, 1982.
[15] A. R. Holzwarth, J. Wendlo, and W. Wehrmeyer, "Picosecond time-resolved energy transfer in phycobilisomes isolated from the red alga porphyridium cruentum," *Biochem. Biophys. Acta*, vol. 724, pp. 388–395, 1983.

Aaron J. Dagen is with the Perkin-Elmer Corporation, Danbury, CT, and is also a Visiting Research Fellow at the Institute for Ultrafast Spectroscopy and Lasers, The City College of New York, New York, NY. The author of seven papers, he expects to receive his doctorate in January 1985.

Robert R. Alfano, for a photograph and biography, see this issue, p. 1342.
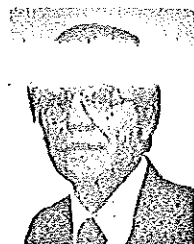
Charles E. Swenberg (M'80) received the Ph.D. degree in condensed matter physics from the Univ. ity of   1968, and did his postdoctoral studies in physics at the University of Illinois, Urbana, IL (1967–1969).

He is currently Chief of the Biological Spectroscopy Division at the Armed Forces Radiobiology Research Institute, Bethesda, MD. Prior to joining the Radiobiology Research Institute, he was a Research Associate Professor of Chemistry at New York University, New York, NY. He has authored or coauthored more than 60 research papers and coauthored both a research text, *Electronic Processes in Organic Crystals* (New York: Oxford), and an undergraduate textbook, *Medical Physics* (New York: Academic).